Synchrotron techniques: x-ray tomography and imaging through diamond anvil cells

Wenge Yang

HPSynC, Geophysical Laboratory, Carnegie Institution of Washington

Advanced Photon Sources, Argonne National Laboratory

XDL – 2011 workshop, CHESS, June 23, 2011

CARNEGIE INSTITUTION FOR SCIENCE

U.S. DEPARTMENT OF ENERGY

Argonne NATIONAL LABORATORY

What can a 3rd/4th generation synchrotron sources provide?

- Continuous spectrum
- High flux
- High brightness
- High coherence
- Polarization
- High energy
- High energy resolution
- Stable source (position, flux)
- Time resolved study

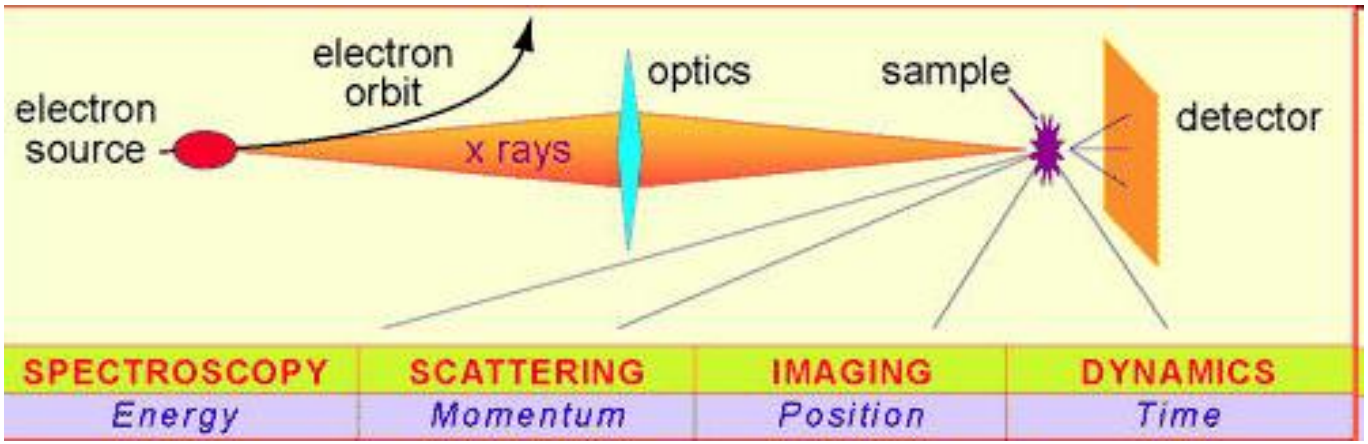

HPSynC

High Pressure Synergetic Consortium at theAdvanced Photon Source

Established in 2007

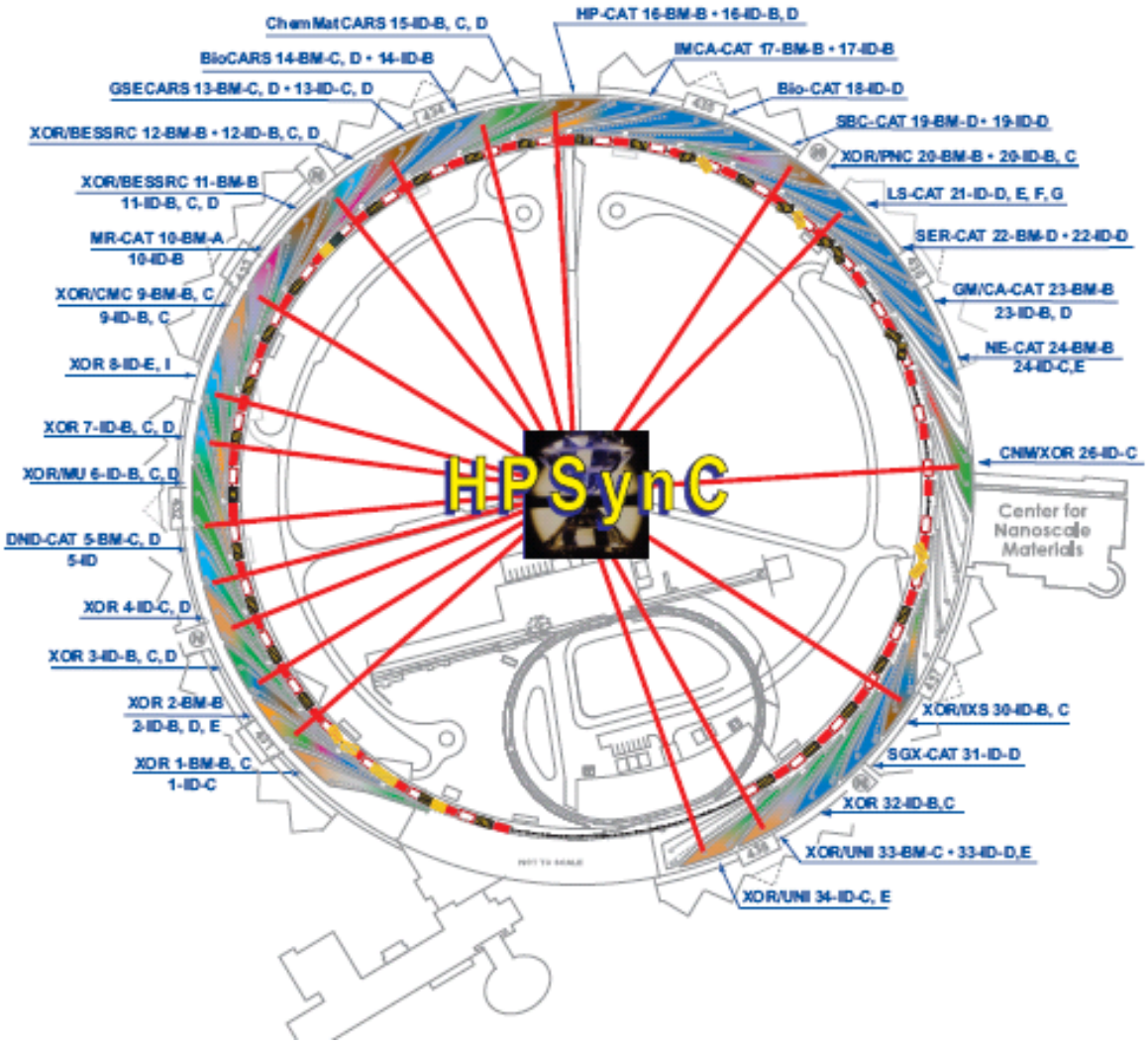

Mission:

develop high risk, high return, high pressure synchrotron sciences and Technologies

current focus Activities

New science and novel HP-SR techniques

Nano imaging (TXM), diffraction

Coherence (CDI)

High energy scattering (PDF)

High energy resolution (HERIX, MERIX)

Various novel spectroscopy

Time resolved (Shock wave, XPCS)

Magnetic study (XMCD)

Nano-diffraction on high pressure

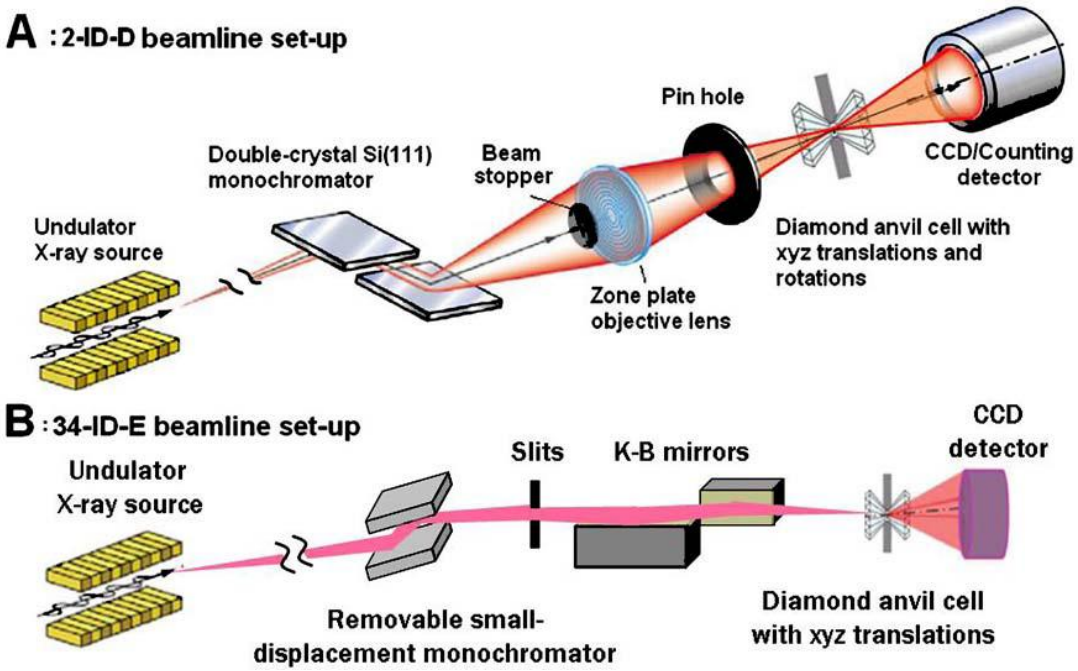

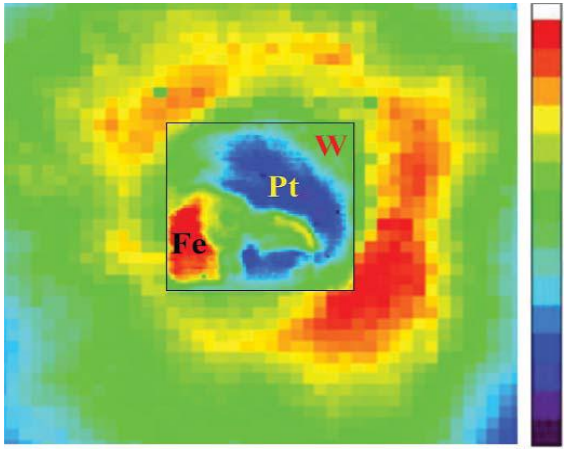

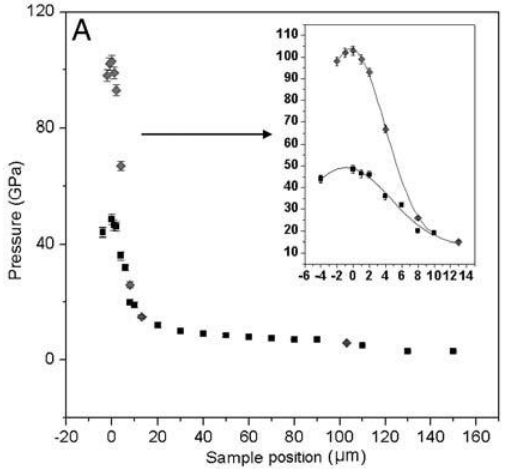

Nano-diffraction beamlines at APS (typical beamsize 200-500 nm)

Nanoprobe measurements of materials at megabar pressures
L. Wang et al. PNAS, 107, 6140 (2010)

Orientation percolation map between substrate and film

2d raster-scan on film and substrate, both crystals diffract simultaneously. Indexing of the individual grain orientation gives the orientation maps and percolative region by small angle grain boundaries.

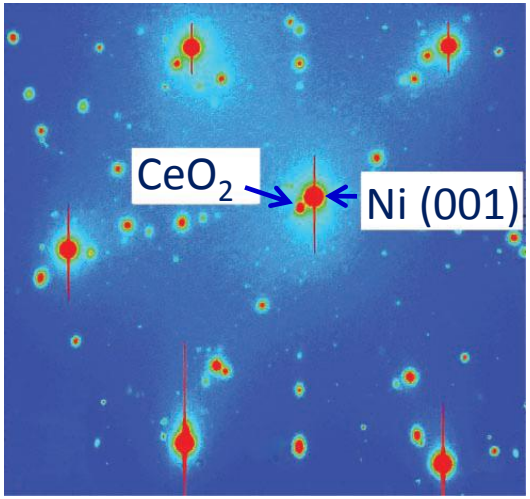

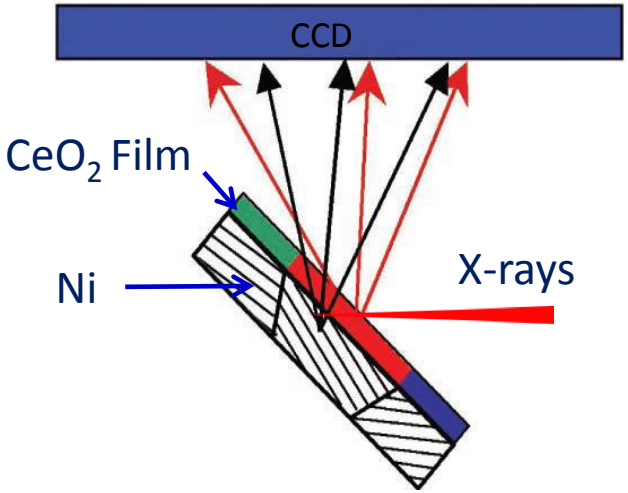

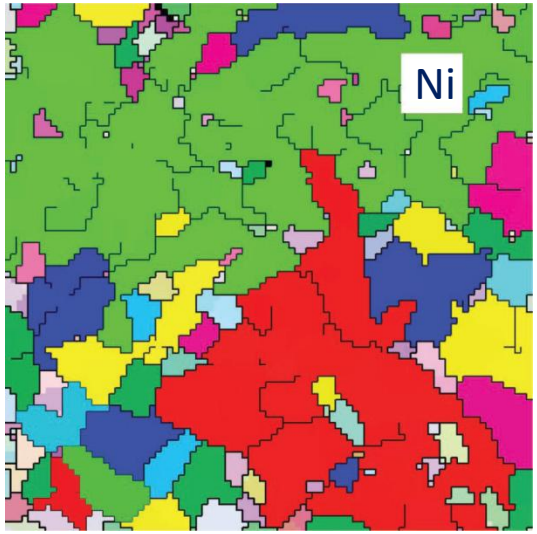

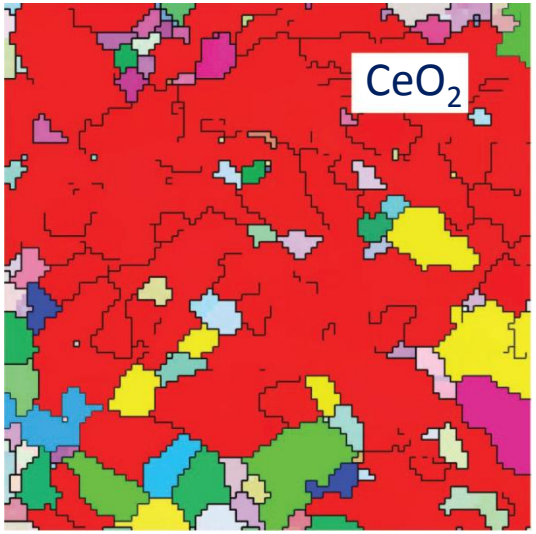

Orientation maps produced by X-ray microdiffraction. Black lines indicate boundaries between pixels where the total misorientation (including both in-plane and out-of plane components) is greater than 5°.Each coloured area shows a percolative region connected by boundaries of less than 5°. J.D. Budai et al., "X-ray microdiffraction study of growth modes and crystallographic tilts in oxide films on metal substrates," *Nat. Mater.* **2**, 487 (2003).

Density measurement for non-crystalline materials in DAC is important

PRL 104, 105702 (2010) PHYSICAL REVIEW LETTERS week ending 12 MARCH 2010

Origin of Pressure-Induced Polyamorphism in $Ce_{75}Al_{25}$ Metallic Glass

Qiao-shi Zeng,[1,2] Yang Ding,[2] Wendy L. Mao,[1,3,4,5] Wenge Yang,[2,6] Stas. V. Sinogeikin,[6] Jinfu Shu,[7] Ho-kwang Mao,[1,2,6,7] and J. Z. Jiang[1,*]

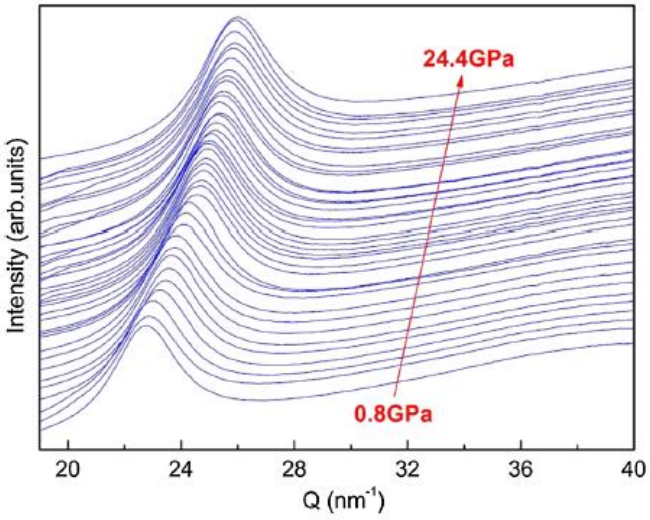

FIG. 2 (color online). *In situ* high-pressure XRD patterns of $Ce_{75}Al_{25}$ metallic glass from 0.8 to 24.4 GPa. The position of FSDP shifts to the higher Q values with increasing pressure as a result of densification.

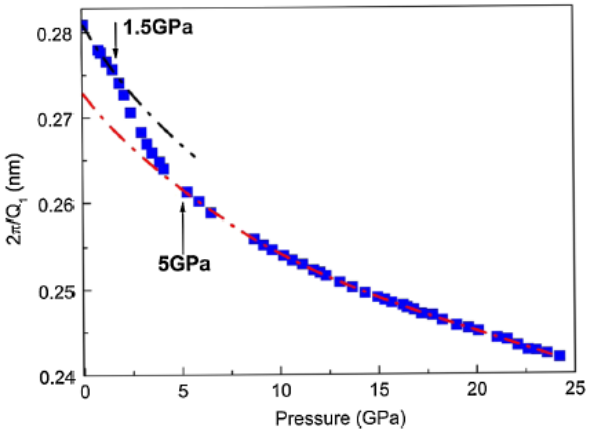

FIG. 3 (color online). Inverse FSDP positions $2\pi/Q_1$ of $Ce_{75}Al_{25}$ metallic glass as a function of pressure. Two distinct states, LDA (dashed black line) and HDA (dashed red line) along with a transition region from about 1.5 to 5 GPa can be identified. The data are smooth owing to the hydrostatic pressure conditions, and the pressure uncertainty is smaller than the symbol size.

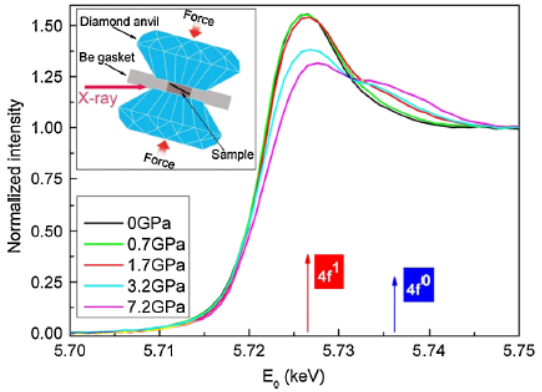

FIG. 4 (color online). *In situ* high-pressure Ce L_3-edge XAS spectra of $Ce_{75}Al_{25}$ metallic glass. The arrows point to the $4f^0$ and $4f^1$ components. The appearance of the $4f^0$ feature indicates the delocalization of $4f$ electron, and coincides with the volume collapse in XRD results. The inset shows a schematic of the *in situ* high-pressure XAS experimental geometry.

Intensity correction:

$$I^{obs}(Q) = PAG[I^{coh}(Q) + I^{inc}(Q) + I^{mul}(Q) + I^{back}(Q)] \quad (1)$$

P: the polarization factor, *A:* the absorption factor, *G:* the geometric factor, I^{coh}, I^{inc}, and I^{mul}: the coherent, incoherent, multiple scattering intensities, I^{back} is the background scattering from the surrounding materials

Equation (1) can be rewritten as a corrected intensity $I^{cor}(Q)=I^{obs}(Q)/PAG$ as

$$\alpha I^{cor}(Q) = I^{coh}(Q) + I^{inc}(Q) + I^{mul}(Q)$$

α is often called normalization constant. With so-called generalized Krogh-Moe-Norman method (also called radial distribution function), α can be determinate by

$$\alpha = \frac{\int_0^{Q_{max}} Q^2 [\{< f^2 > + I^{inc}(Q) + I^{mul}(Q)\} \frac{\exp(-\gamma Q^2)}{< f >^2}] dQ - 2\pi^2 \rho_0}{\int_0^{Q_{max}} Q^2 [I^{cor}(Q) \frac{\exp(-\gamma Q^2)}{< f >^2}] dQ}$$

Here, ρ_0 is the average number density of the sample, and an artificial damping factor $\exp(-\gamma Q^2)$ is introduced to reduce the error from large Q regions. Following the Faber-Ziman form, the coherent scattering intensity is given by the following equations,

$$I^{coh}(Q) = < f^2 > + < f >^2 \int_0^{\infty} 4\pi r^2 [\rho(r) - \rho_0] \frac{\sin(Qr)}{Qr} dr$$

$$S(Q) = [I^{coh}(Q) - (< f^2 > - < f >^2)] / < f >^2$$

Schematic of the TXM setup at APS 32ID-C, SSRL 6-2

3d Nano-imaging

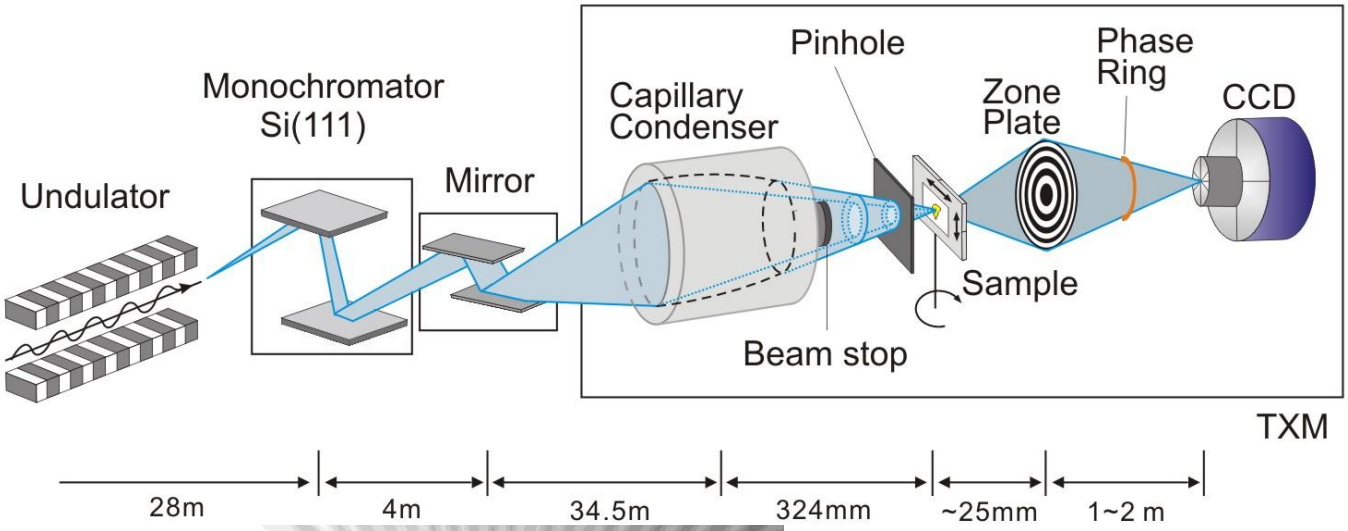

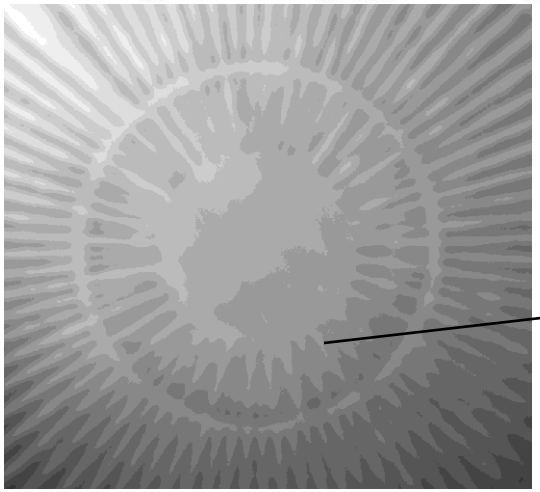

30 nm feature

TEM

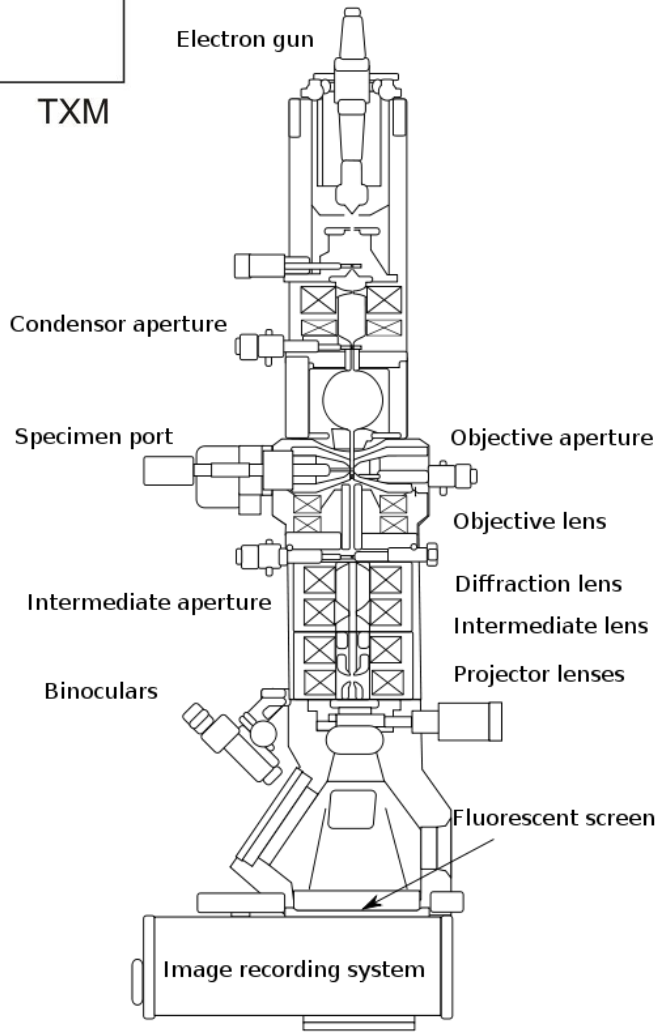

Beamline capabilities:
Full field imaging with 180 degrees data collection; 3d reconstruction with FOV 25 microns and 30 nm require uniform illumination for FOV (diffuser sometimes is used to create incoherent uniform beam)

Iteration method to overcome the missing angle problem

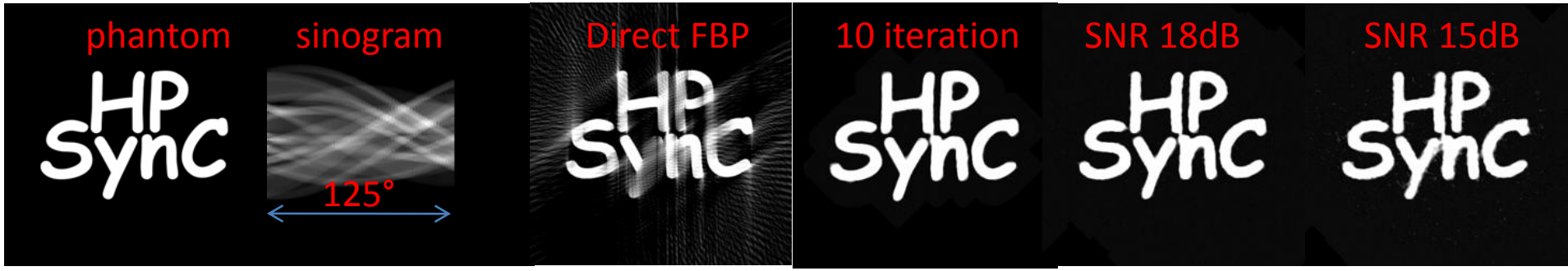

Error reduction

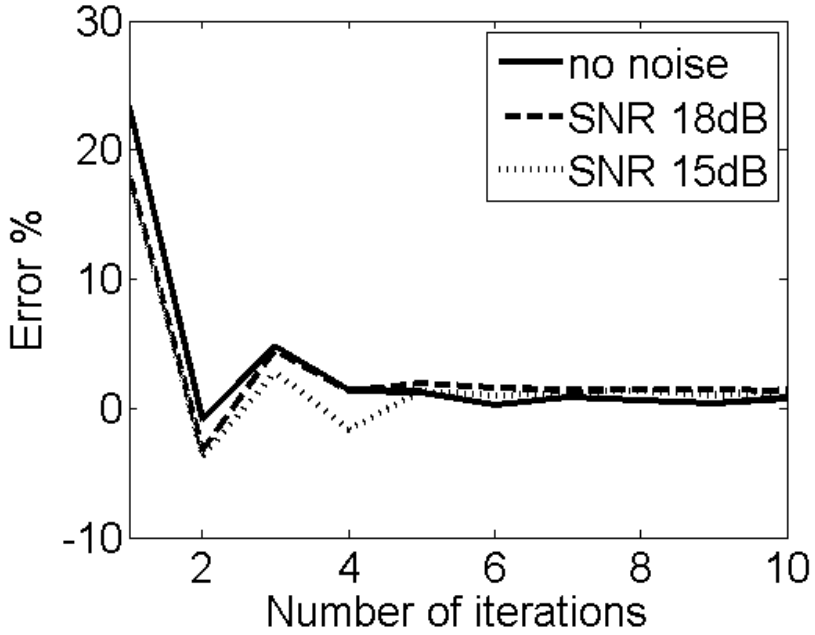

Missing angle issue

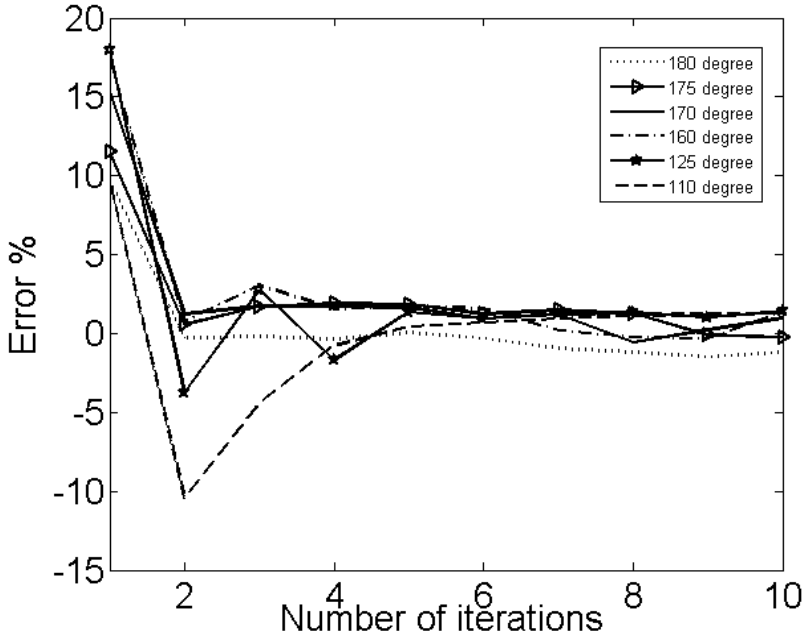

Case study of sample Sn crossing phase transition

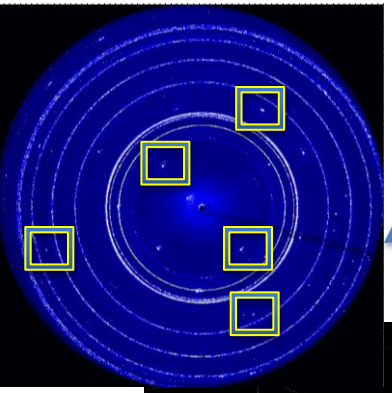

Single crystal diff.
(β-tin)

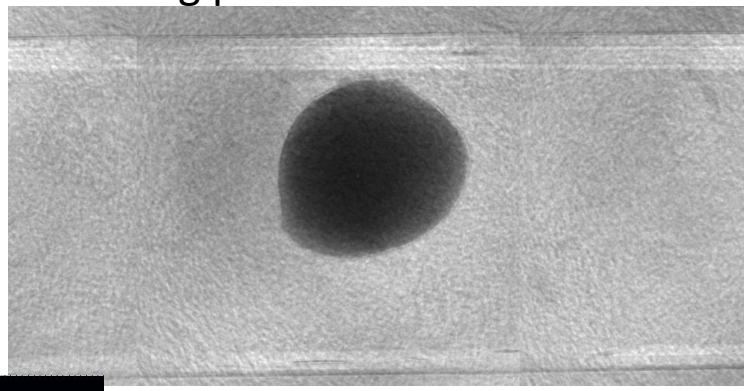

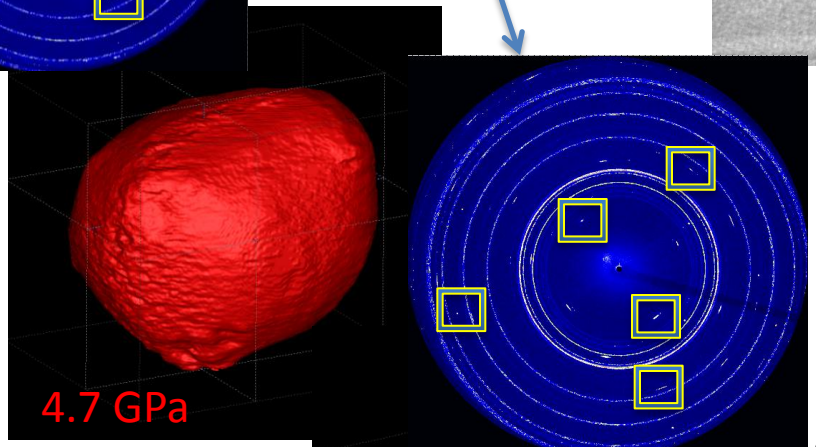

3d reconstructed objects

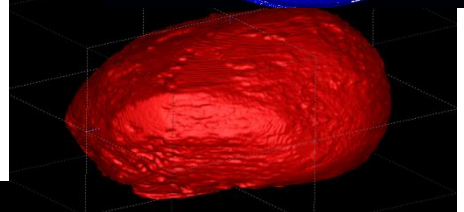

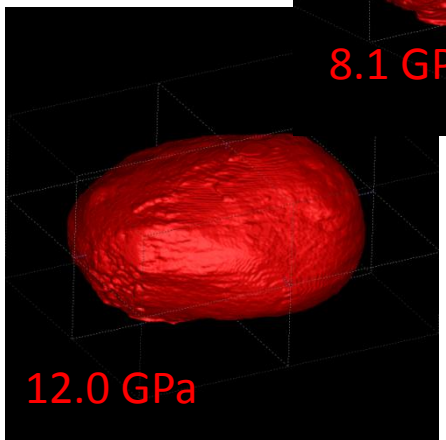

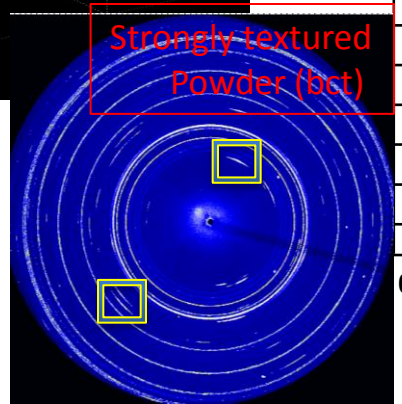

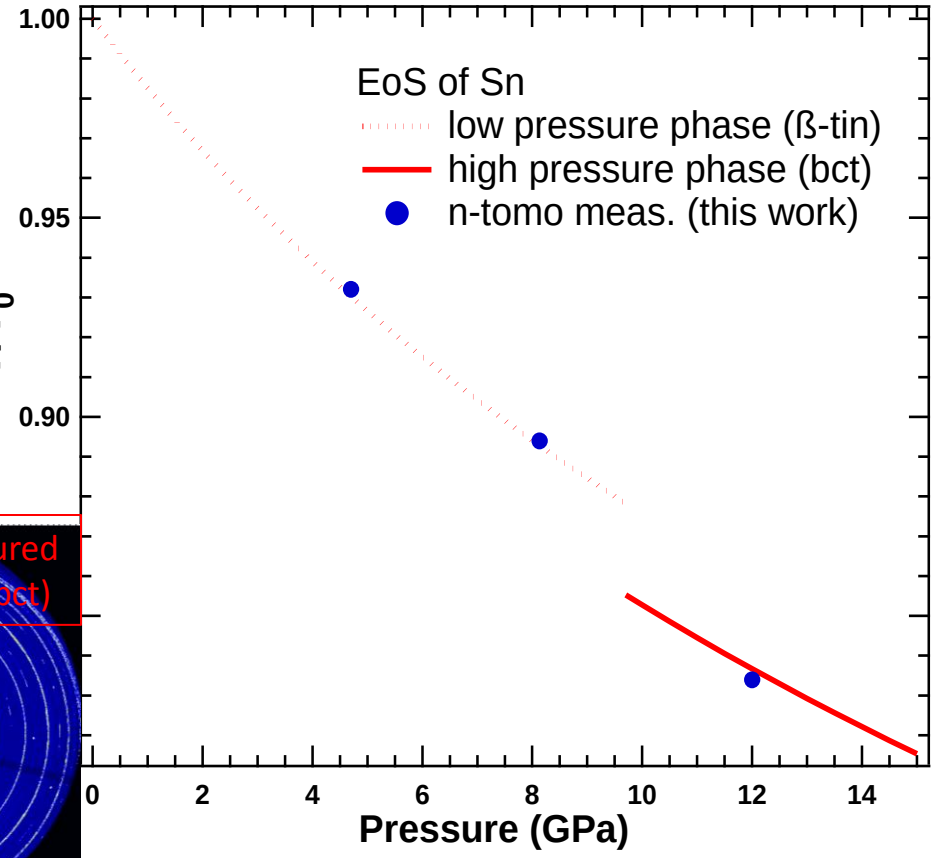

XANES type 3d tomography to map chemical composition

FeNiS in $MgSiO_3$

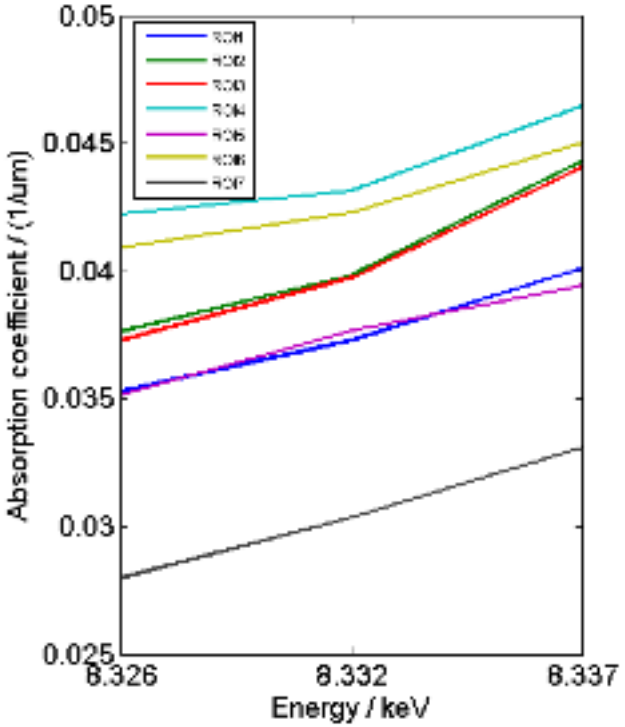

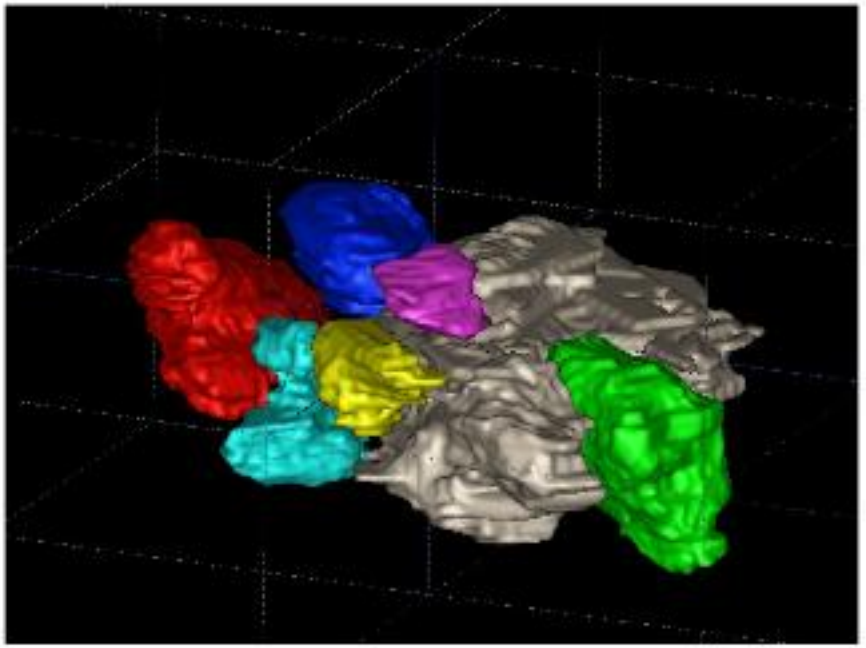

Bragg Coherent diffraction

Coherent diffraction imaging (CDI) on single crystal under high pressure

Experimental setup at 34ID-C, APS

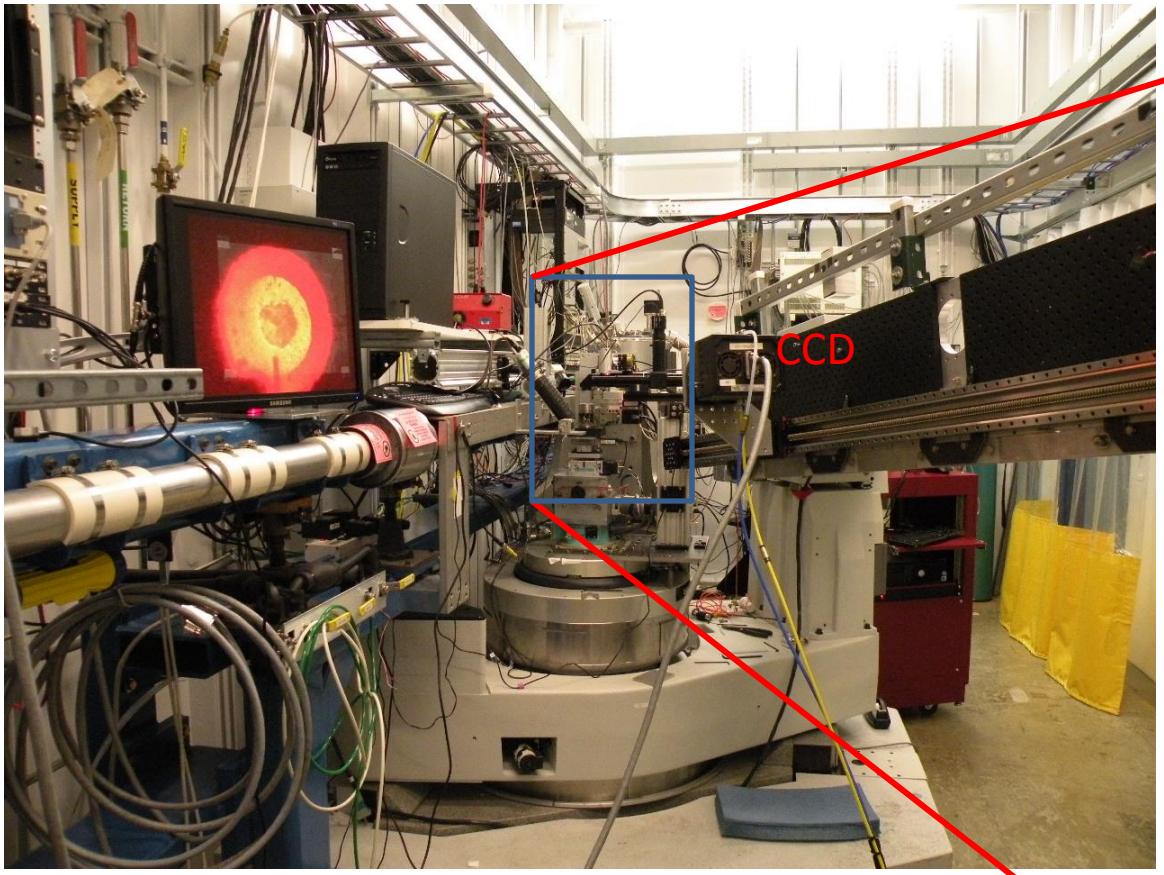

Panoramic DAC on
a kinematical mount

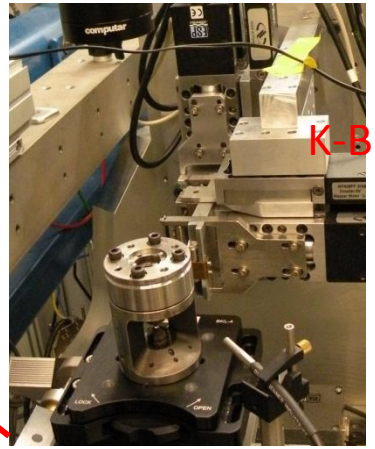

K-B Mirrors

Sample: ~ 300 nm diameter gold single crystal on 15 um thick Si wafer

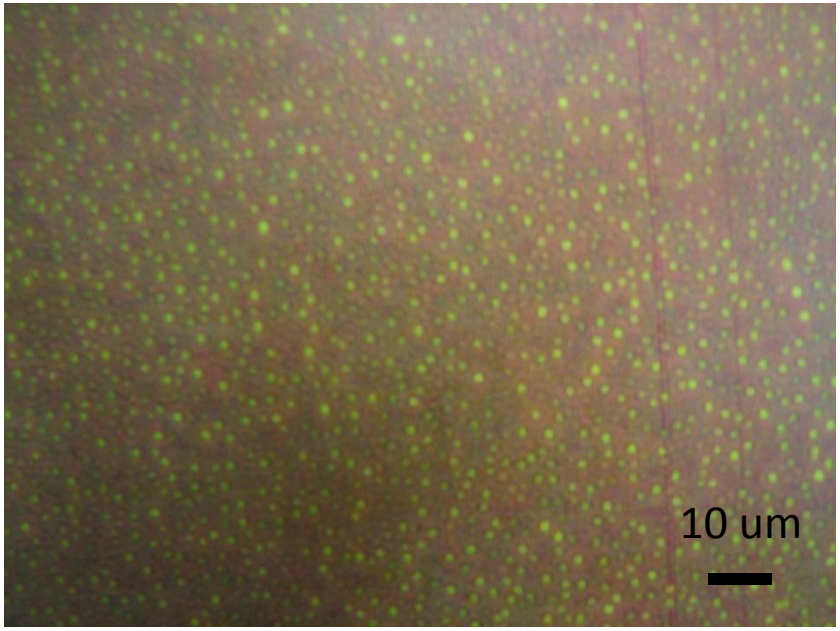

Average 300 nm size Au single crystals grown on Si wafer

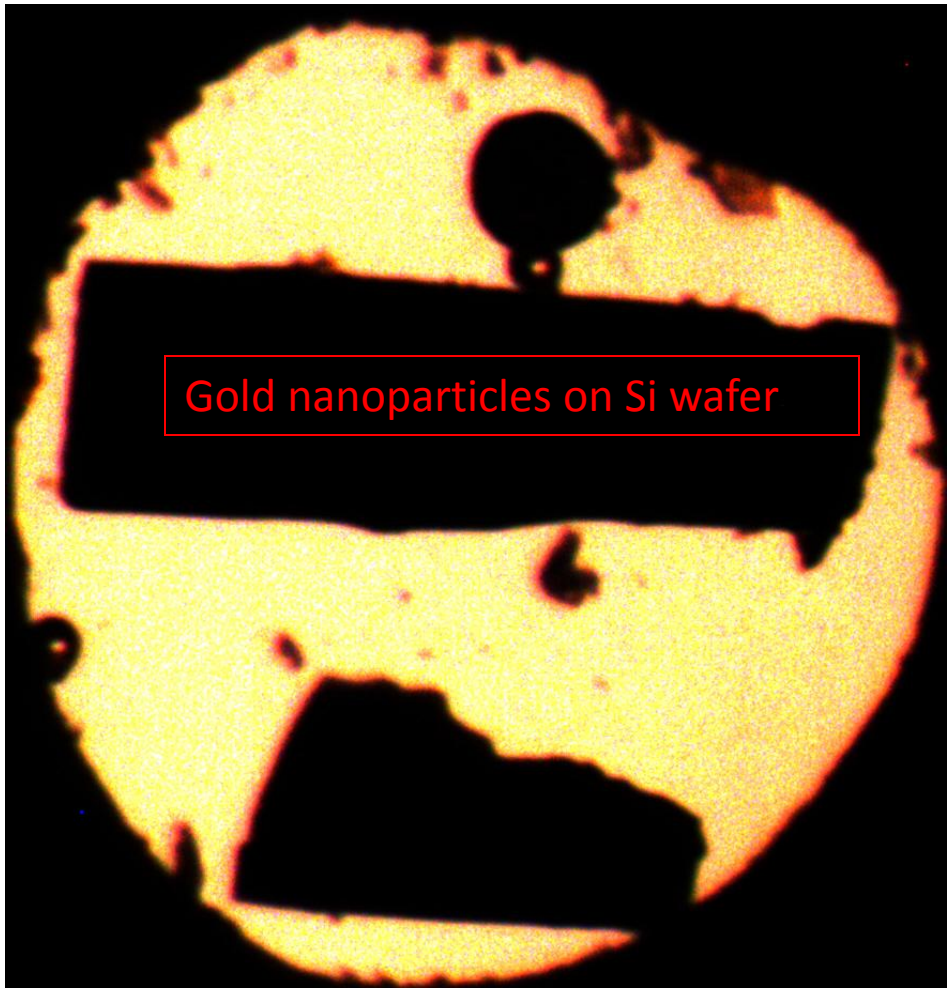

Phase retrieval algorithm

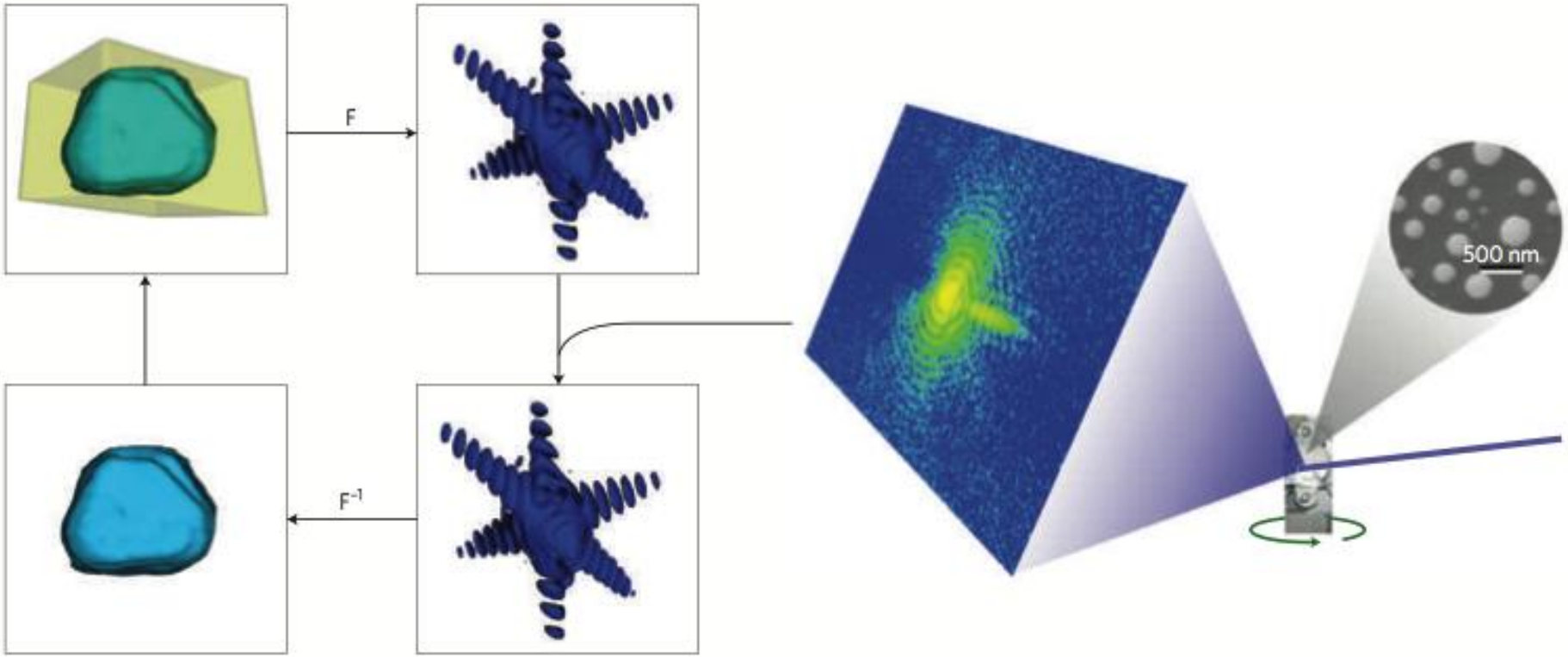

I Robinson and R. Harder, Coherent x-ray diffraction imaging of strain at the nanoscale, Nature Materials 8, 291 (2009)

3d reconstruction of magnitude and phase

magnitude

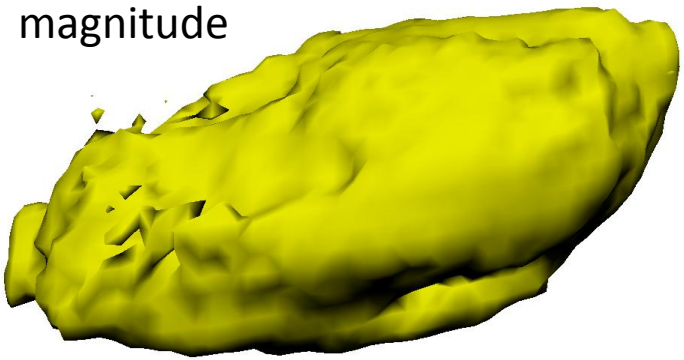

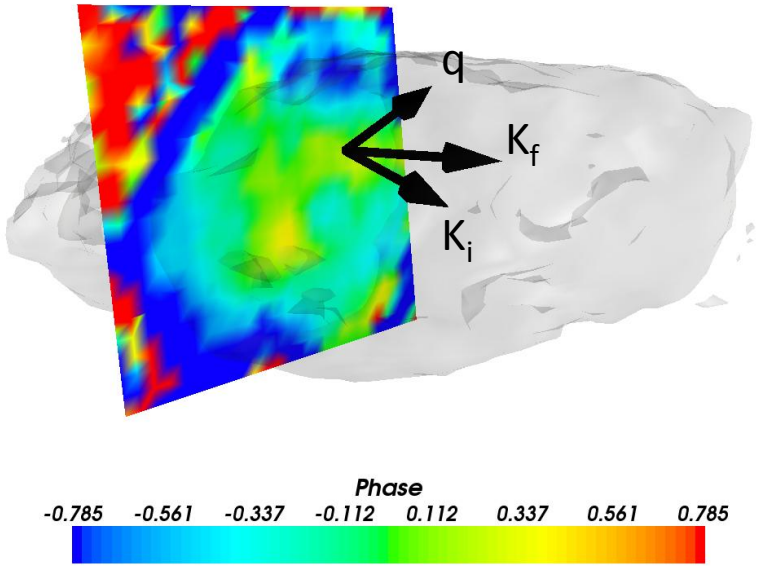

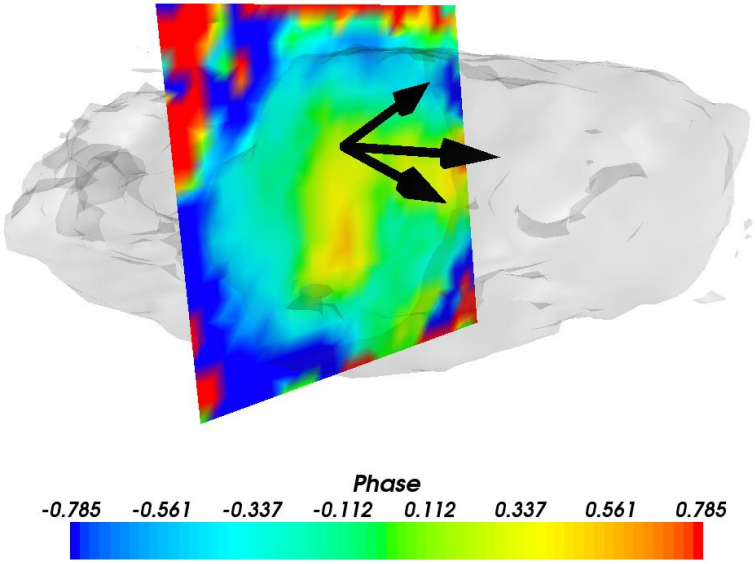

phase

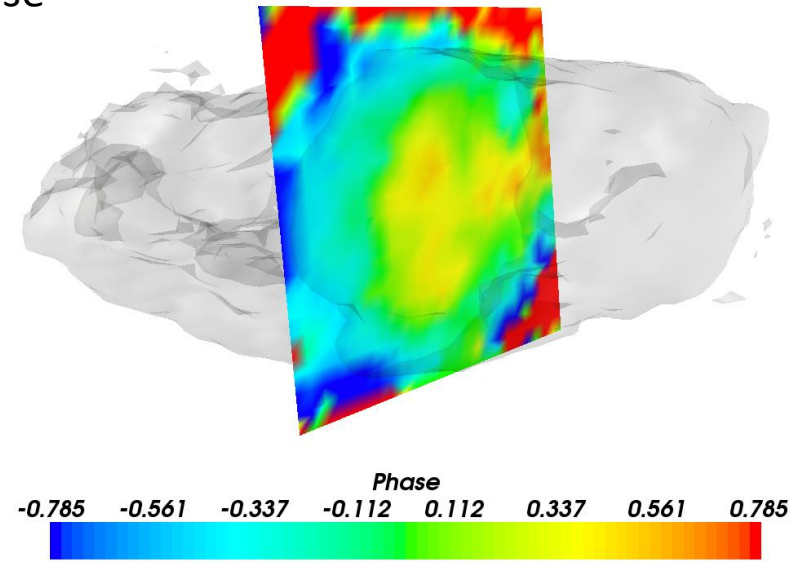

Phase contrast represents the strain in side of the nano-particle

High-pressure/density phase transitions by femto second laser shock

(2007-10 Kaken, Japan; 2009-11 Discovery, Australia)

Single-shot dielectric breakdown

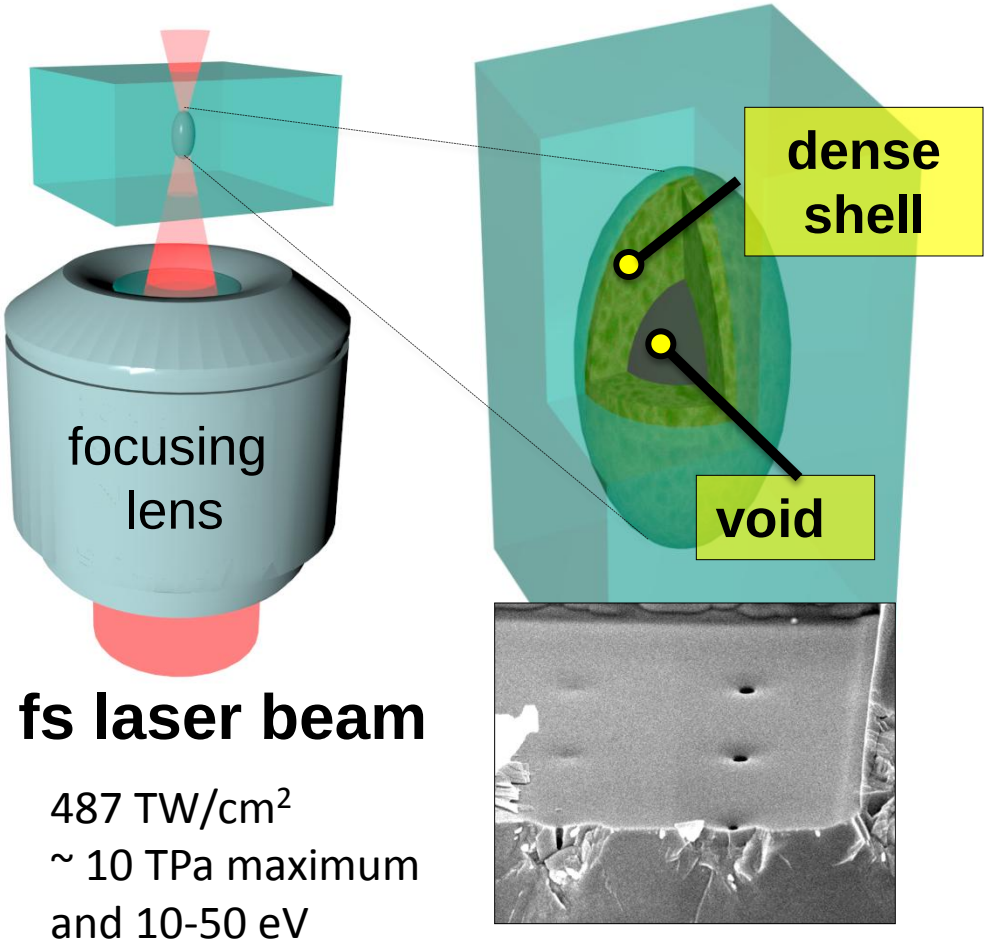

fs laser beam

487 TW/cm^2
~ 10 TPa maximum
and 10-50 eV

100nJ/200fs/800nm

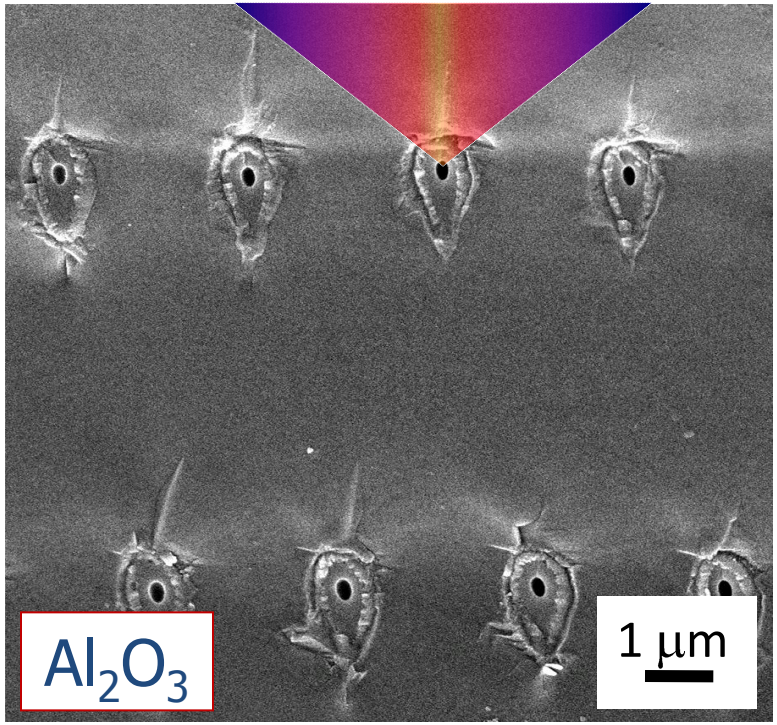

Phys.Rev.Lett. 96 166101 2006
Phys.Rev. B 73 214101 2006

Femto second laser shock

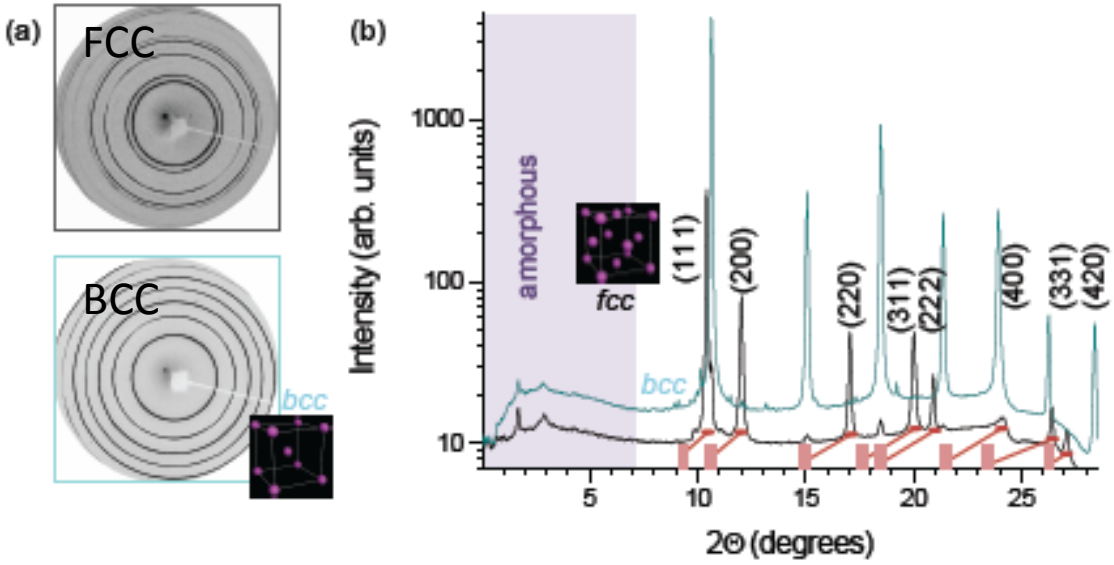

Shock dynamics

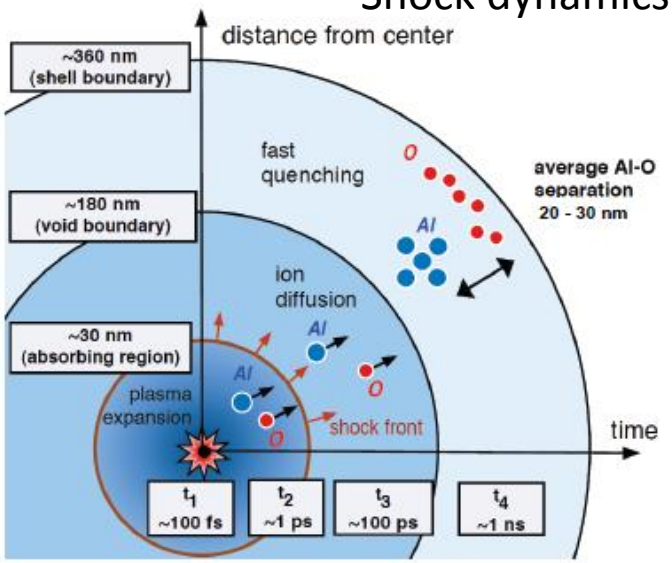

Theoretical prediction of Al under high pressure
Pickard and Needs,
Nat.Materials 9, 624(2010)

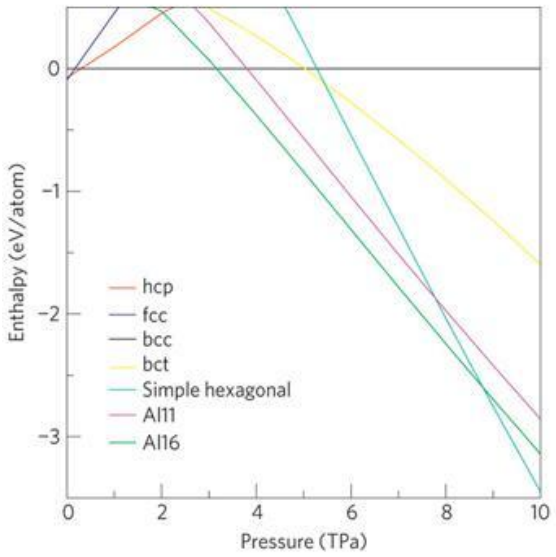

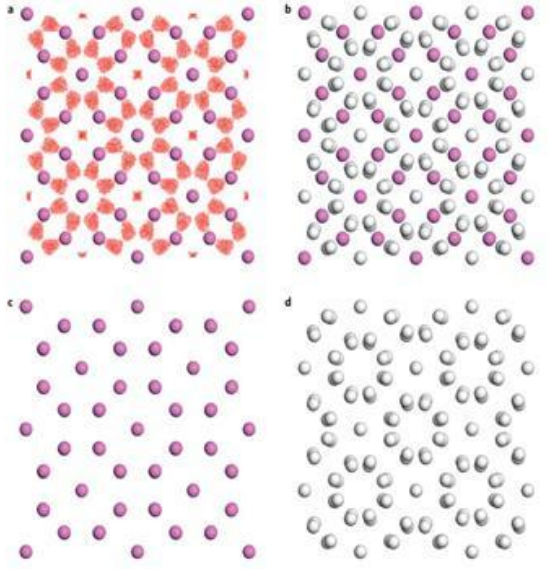

Al16 model

Nature Communication (2011)

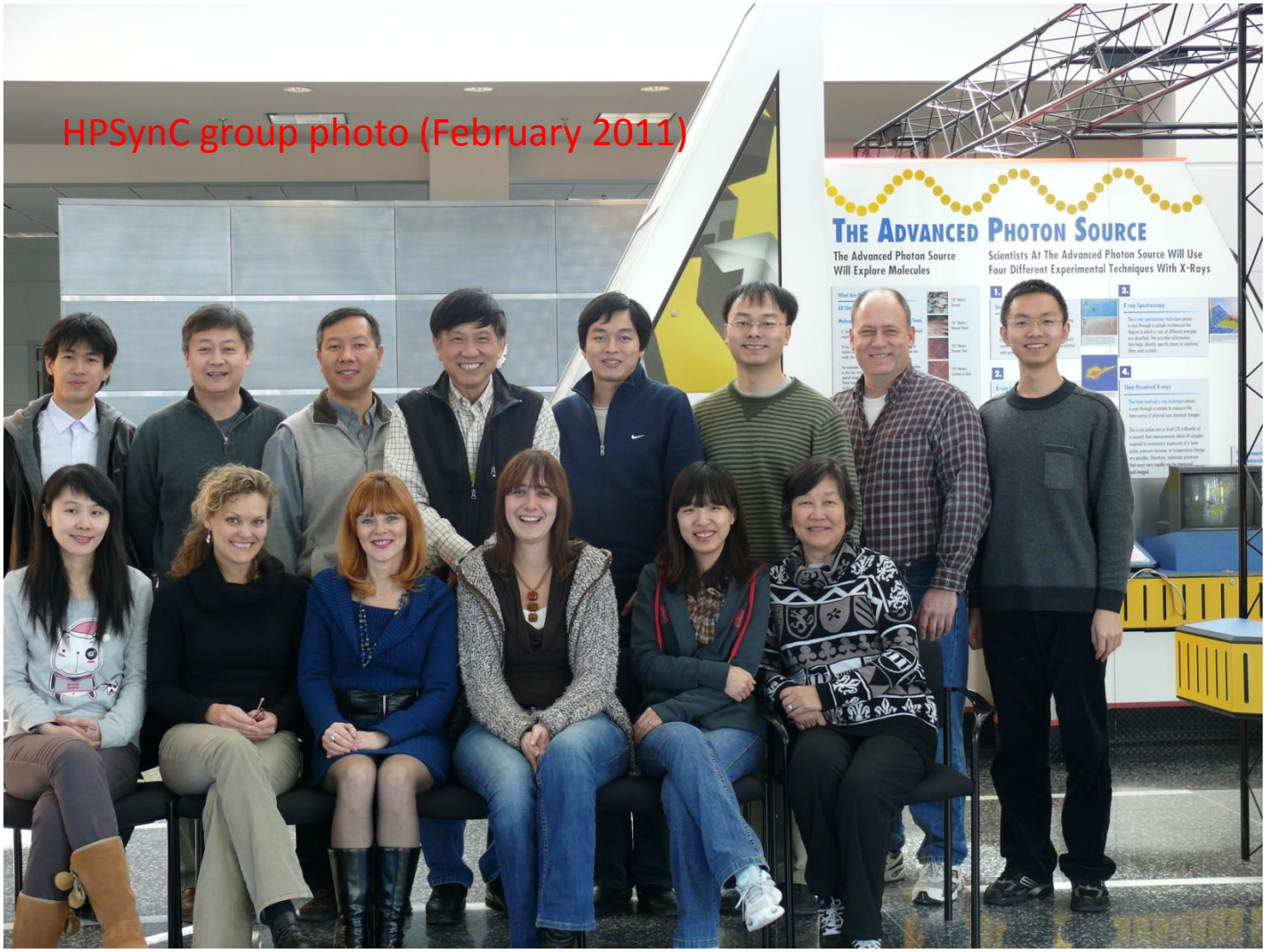
HPSynC group photo (February 2011)
THE ADVANCED PHOTON SOURCE
The Advanced Photon Source Will Explore Molecules
Scientists At The Advanced Photon Source Will Use Four Different Experimental Techniques With X-Rays

ERL for HP studies

Advantages of an ERL source (after Bilderback, New Journal of Physics)

Outstanding coherent flux - The ERL will produce outstanding coherent flux The ERL will produce outstanding coherent flux…for example at 10 keV, the 25 m ERL Delta undulator (see section 3.3) will produce about 2.4 E14 coherent photons s−1/0.1% bw, about 100 times higher than NSLS-II 3 m ID-U20, and 1500 times that of APS undulator-A, and will exceed all sources up to 60 keV.

Round beams - An ERL with near-isotropic transverse emittance will have an approximately round source that is ideal for coherent scattering because the horizontal and vertical transverse coherence lengths will be matched.

Flexibility - Unlike a storage ring, ERL electron beam transport optics need not be periodic for multi-turn storage and there is no separate injection orbit, so advanced insertion devices like the ERL Delta undulator (with small gap in both horizontal and vertical directions) will offer unique beam properties.

Quasi-continuous time structure - Because of the short pulse length (2 ps RMS) and high repetition rate (1.3 GHz), the ERL time structure will be closer to that of a continuous source than at storage rings.